



## Vertical post-tensioned connection for modular steel buildings

Rafaela Sanches<sup>1</sup>, Oya Mercan<sup>2</sup>

<sup>1</sup> Ph.D. Student, Department of Civil and Mineral Engineering, University of Toronto – Toronto, ON, Canada.

<sup>2</sup> Associate Professor, Department of Civil and Mineral Engineering, University of Toronto – Toronto, ON, Canada.

### ABSTRACT

Modular construction is a construction technique where prefabricated volumetric modules are prepared in a factory and assembled on-site to form permanent buildings. Typically, vertical connections between modules are provided using on-site welding. However, welding may interfere with the finishing of the modular units, and once the modules are placed next to each other the access to all sides of the columns can be limited resulting in partial welding in the vertical connections. This paper investigates a new vertical intermodular connection for modular steel buildings (MSBs). The connection consists of a post-tensioned (PT) threaded steel rod that is installed inside hollow section columns together with a steel box that is inserted between two columns. Experiments were performed to assess the performance of the proposed connection and compare it with a typical welded connection. Eurocode 3 Part 1–8 was used to classify the connection by stiffness and strength. The results showed that the PT connection has lateral stiffness comparable to the welded connection; it presents higher energy dissipation capability, and it can be classified as a partial strength semi-rigid connection. Furthermore, both welded and PT specimens have adequate ductility and withstand up to 3% drift without welding fractures or buckling. Vertical PT connection has the potential to substitute typical on-site intermodular welded connection; therefore, it will contribute to the development of the modular construction industry.

Keywords: Modular steel buildings, post-tensioned connection, cyclic displacement tests, ductility, Eurocode 3 Part 1-8.

### INTRODUCTION

As an alternative to conventional construction techniques, modular construction is a method in which prefabricated volumetric modules are fully finished at a factory in a controlled environment and assembled on-site to form a larger permanent building. More suitable for buildings with repeatable units - for instance schools, residential buildings, and military facilities - modular construction has gained popularity due to the improved quality and speed of installation leading to cost and time savings, as well as due to the reduction of material waste [1-3].

Despite the increasing number of modular steel buildings (MSBs) [4,5], relatively few studies have investigated their dynamic behavior. Both experimental and numerical analyses were performed by Annan et al. [6,7] to evaluate ductility and overstrength factors for multistory MSBs. It was concluded that MSBs present stable and ductile behavior, and significant overstrength. Fathieh and Mercan [8] performed numerical dynamic analysis in a 4-story MSB with typical welded connection. They reported a high base shear capacity for MSBs due to the increased number of columns in comparison to conventional buildings. Gunawardena [4] investigated the seismic performance of a 10-story MSB with bolted connection and stiffened modules. The results showed that under severe earthquakes the columns formed hinges.

On-site welding is typically used for vertical intermodular connection (i.e., connection between modules). However, the access to weld the columns is limited once one module is positioned next to the other. This leads to partial welding which may cause undesirable relative rotation between modules [6]. To substitute on-site welding, alternative types of connections have been proposed for both conventional and modular steel structures. Ricles et al. [9,10] and Garlock et al. [11,12] studied the use of post-tensioned (PT) steel strands for horizontal beam-column connection of typical steel frames. They showed that horizontal PT connection eliminates on-site welding, improves the dynamic performance of the structural system, and has initial stiffness similar to that of a typical welded connection. Chi and Liu [13] investigated the cyclic response of a vertical column base with PT connection. The vertical PT connection presents stable hysteretic behavior and negligible residual deformation. A vertical prestressed connection for MSB with composite columns was investigated by Chen et al. [14]. The results of quasi-static cyclic tests showed that the proposed connection provides adequate lateral load-bearing and ductility. Chen et al. [15,16] performed cyclic displacement tests on full-scale specimens to investigate the performance of an innovative bolted connection for MSBs. It was shown that the connection eliminates on-site welding and provides the lateral capacity required. Similarly, Deng et al. [17] experimentally investigated the hysteretic behavior of a bolted connection for MSB by testing full-scale specimens under

quasi-static cyclic displacements. The results showed that the proposed connection withstands large inter-story drifts without failing and it is categorized as semi-rigid connection according to the Eurocode. Sanches et al. [18] proposed a PT connection for MSBs vertical intermodular connection. A series of quasi-static cyclic displacement tests were performed in full-scale subassemblies to assess the hysteretic behavior, deformation pattern, strain distribution, and stiffness degradation; and compare the behavior of the proposed PT connection with typical welded column-column connection. The results showed that the proposed PT connection has similar initial stiffness to that of welded connection and it withstands up to 3% drift without experiencing welding fractures. The present paper complements the findings reported by Sanches et al. [18] by providing ductility ratio, damping ratio and the Eurocode classification of the tested connections.

### PROPOSED VERTICAL POST-TENSIONED CONNECTION

The proposed connection eliminates on-site welding and it is applicable for modules that have hollow steel section (HSS) columns. The PT connection consists of a threaded steel rod installed inside the columns and anchored against end plates to provide vertical connectivity between the modules. In addition, a hollow steel box with sloped sides is placed inside the columns covering the full height of the two layers of beams and providing horizontal connectivity to the modules (Fig.1). The contact between the outer surface of the steel box and the inner surface of the HSS column provides friction force that contribute in the resistance of tensile forces that may occur in an earthquake event. Steel couplers can be used to join multiple rods allowing the rod to cover a longer height and connect several columns. The proposed connection eliminates on-site welding for vertical column-column connection. Horizontal intermodular connection is typically bolted [5], and beam-column connection is provided by off-site welding when the modular are prepared at the factory.

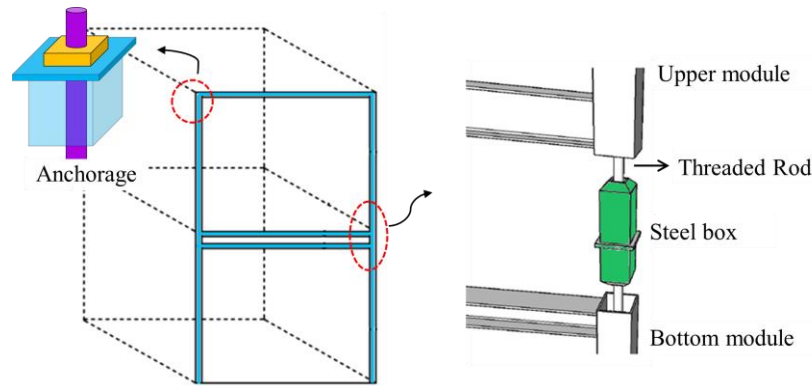


Figure 1. Proposed vertical post-tensioned connection for modular steel buildings.

### SPECIMENS AND TEST SETUP

The specimens tested represent the connection of the first story of a four story MSB (Fig.2a) that was previously studied by Fathieh and Mercan [8]. The thickness of the column was adjusted to improve the stability of the set-up, and the clearance between the floor and ceiling beam was adapted to consider current practices in the modular construction sector. The dimensions of the specimens were determined based on inflection points of the modular building (Fig.2b) and the corresponding boundary conditions were considered. Figure 2c shows the dimensions of the specimens as well as the direction of the displacement applied ( $+\Delta$ ,  $-\Delta$ ) and the constant axial load ( $V$ ). Beam-column connection was provided by typical fillet welding and fabricated at a modular construction factory in Grimbsy, Ontario. The steel box total height covers the height of the two layers of beam at each story level. Ten full-scale T-shape subassemblies were tested under quasi-static cyclic displacements according to AISC protocol [19]. Eight specimens were tested with the proposed PT connection and two were tested with typical column-column welded connection. Appropriate boundary conditions were considered at both columns and beams ends, as indicated in Figure 2c. The base of the bottom column was attached to a spherical support which allowed rotations, but restrained translations, corresponding to a pinned support. At the end of each beam a roller support was considered such that only in-plane rotation and translation along the centerline of the beams were allowed. A free end was considered at the top end of the upper column by combining a spherical support and rollers.

A general view of the test setup is shown in Figure 3a. Quasi-static lateral cyclic displacements were applied at the end of the upper column by a hydraulic actuator with maximum stroke of  $\pm 127$  mm. The displacement protocol is indicated in Figure 3b, where  $\Delta$  is the displacement and  $\gamma$  is the equivalent drift, which is the ratio of displacement  $\Delta$  to the total length of the column (3345mm). In addition, constant axial load ( $V$ ) of 100 kN was applied by a hydraulic jack mounted at the end of the bottom column to represent the gravity load due to concrete floor and insulation ( $2.25 \text{ kN/m}^2$ ), superimposed dead loads for floor ( $0.75$

kN/m<sup>2</sup>), roof (0.32 kN/m<sup>2</sup>) and ceilings (0.7 kN/m<sup>2</sup>), live load (1.9 kN/m<sup>2</sup>) and snow load (1.1 kN/m<sup>2</sup>). Specimens tested with the PT connection were assembled with a 25.4 mm of diameter steel threaded rod anchored against end plates. The initial posttensioning load (PT<sub>0</sub>) applied to the rod varied from 0 kN to 80 kN.

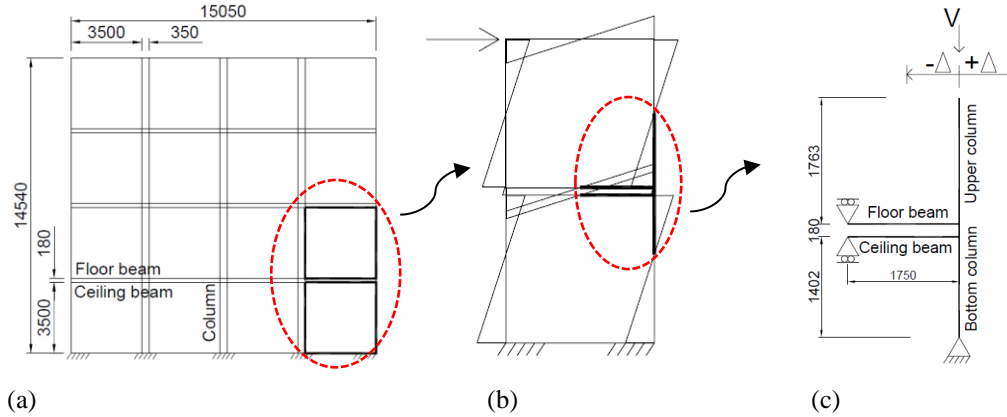


Figure 2. (a) Four story MSB, (b) Inflection point, (c) Specimen centerline dimensions in mm.

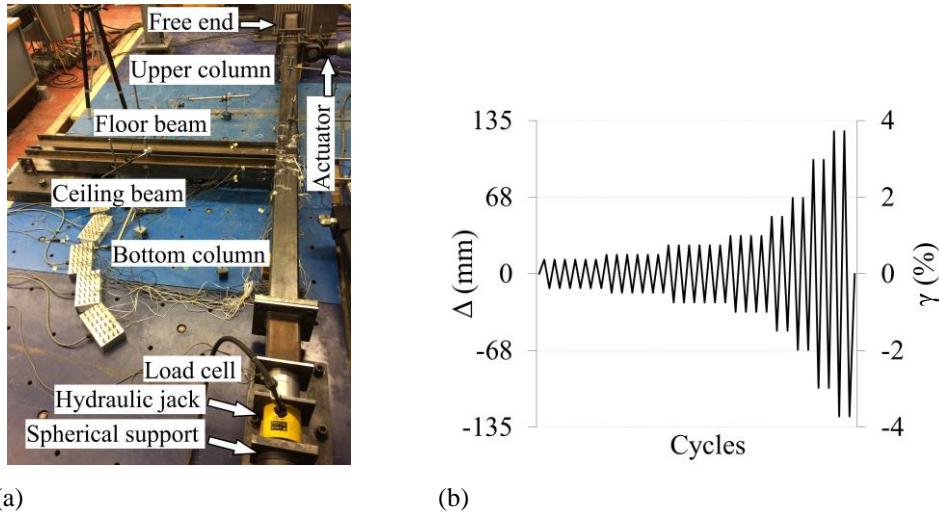


Figure 3. (a) Test setup, (b) Displacement protocol.

The cross sections and material properties of the columns, beams, and steel boxes are indicated in Table 1. Three coupons per batch were tested according to ASTM-A370 [20] to obtain yield stress ( $f_y$ ), ultimate stress ( $f_u$ ), yield strain ( $\epsilon_y$ ) and Young's modulus ( $E$ ) of the specimen's material. All coupons were cut from flat surfaces in the longitudinal direction. Beams were produced from ASTM A572 Gr50, and the columns and steel boxes were from CSA G40.21-350W Class C. The test matrix is indicated in Table 2, showing specimens name, the type of steel box considered, the initial posttensioning load (PT<sub>0</sub>), the maximum displacement ( $\Delta_{max}$ ) applied by the actuator and equivalent maximum drift ( $\gamma_{max}$ ) for each specimen. Specimens R2W and R4W were tested with partial welding and all-around welding for vertical connection of columns, respectively. To evaluate the performance of the proposed PT connection eight tests were performed in specimens with different steel box thicknesses (B1, B2, and B3) and PT<sub>0</sub> loads (0 kN, 60kN and 80 kN). The thicknesses of the steel boxes were chosen to be proportionate to the column thickness, and maximum PT<sub>0</sub> was selected such that the total axial load acting in the column did not exceed the buckling load. The specimens tested with the PT connection were named based on the steel box thickness considered and the PT<sub>0</sub> load applied. For instance, the specimen B1PT60 was tested with the steel box B1 and PT<sub>0</sub> of 60 kN. One of the PT specimens was tested with a coupler connecting two parts of the threaded rod (B1PT80C) to investigate the connection performance when longer rods are required to connect multiple modules. Two PT specimens were retested with increased PT<sub>0</sub> load: B1PT0 was retested as B1PT60, and B3PT60 was retested as B3PT80. Additionally, in order to assess the performance of the PT connection in case of unexpected loss of PT load, two specimens (B1PT0 and B3PT0) were tested with zero PT<sub>0</sub> load. The 100 kN constant axial load was maintained for all tests. Both the threaded rod and the coupler are composed of high strength steel Grade 8 [21]. To obtain the deformed shape of the specimen ten Linear Variable Differential Transformers (LVDTs) were placed along the column length and at middle of the beams to measure in-plane displacements and out-of-plane deflections. More details on the instrumentation and test setup are reported in [18].

Table 1. Cross section and material properties.

Element		Cross section	$f_y$ (MPa)	$f_u$ (MPa)	E (MPa)	$\epsilon_y$ (%)
Column		HSS 127x127x6.4	372	450	193,350	0.39
Threaded rod		Ø 25.4	986	1081	202,086	0.69
Floor beam		W 150x18 (Flange)	351	510	193,652	0.20
		W 150x18 (Web)	390	532	197,463	0.19
Ceiling beam		W 100x19 (Flange)	331	478	202,247	0.19
		W 100x19 (Web)	371	504	196,213	0.19
Steel box	(B1)	HSS 102x102x6.4	406	469	209,738	0.40
	(B2)	HSS 102x102x9.5	411	460	185,706	0.42
	(B3)	HSS 102x102x12.7	432	475	185,824	0.44

Table 2. Test matrix.

Specimen	Steel Box	PT <sub>0</sub> (kN)	$\Delta_{max}$ (mm)	$\gamma_{max}$ (%)	Observation
R2W	-	-	± 66.90	± 2.0	2 sides welded
R4W	-	-	± 125.44	± 3.7	4 sides welded
B1PT0	B1	0	± 100.35	± 3.0	-
B1PT60	B1	60	+ 125.44 / -100.35	+ 3.7 / - 3.0	-
B1PT80	B1	80	± 125.44	± 3.7	-
B1PT80C	B1	80	± 125.44	± 3.7	with couplers
B2PT80	B2	80	± 125.44	± 3.7	-
B3PT0	B3	0	± 125.44	± 3.7	-
B3PT60	B3	60	± 125.44	± 3.7	-
B3PT80	B3	80	± 125.44	± 3.7	-

## RESULTS AND ANALYSIS

### General connection behavior

As discussed previously, the access to weld all sides of the columns may be limited during the assembly process of the modules. Therefore, a partially welded specimen (R2W) was tested up to  $\pm 2\%$  drift. Neither weld fracture nor buckling were observed. Then, the specimen was fully welded (all four sides of the columns were welded) as indicated in Fig.4a, renamed as R4W and retested up to  $\pm 3.7\%$  drift. A small weld fracture was observed in the floor beam-column connection at 3% drift (Fig. 4b), but no buckling was noticed. Eight tests were carried out in specimens with PT connections. The first two PT specimens tested, B1PT0 and B1PT60, presented instability issues as the drift exceeded 3%. Thus, the maximum displacement applied to these two specimens were smaller than to the others, as indicated in Table 2. All other PT specimens were tested up to  $\pm 3.7\%$  drift. Except specimen B2PT80, a weld fracture was observed in the floor beam-column connection when the drift exceeded 3% (Fig.4c). At -3% drift a gap between upper column and mid-plate of the steel box was observed (Fig.4d), except for specimens with PT<sub>0</sub> = 0 kN in which the gap could be seen at -1% drift. It is worth mentioning that the gap opening occurred only for negative displacements ( $-\Delta$ ). As expected, with increased PT<sub>0</sub> load the gap opening decreased and the deformed shape of the specimen approximates the deformed configuration of the welded one [18]. The use of the coupler did not alter the deformed shape of the specimen.

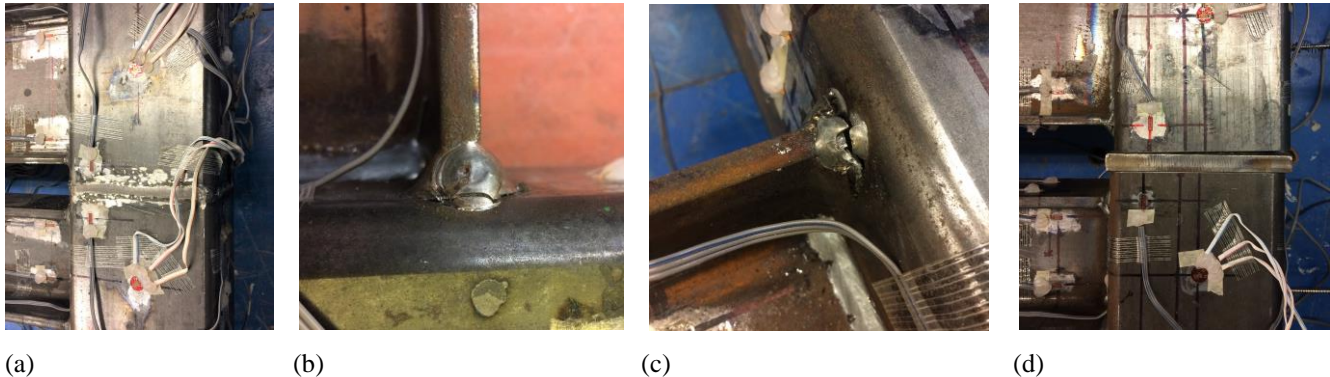


Figure 4. (a) Welded column-column connection (R4W); Weld fracture in the floor beam-column connection of (b) R4W and (c) B3PT80; (d) Gap opening at -3.7% drift (B3PT0).

**Hysteretic behavior, skeleton curves and ductility**

Hysteretic curves for PT specimens are similar to that of welded specimens, as illustrated in Fig.5a. The skeleton curves show the peak load at each set of cycles and the respective drift applied. Skeleton curves shown in Fig.5b indicate that, in general, PT specimens with thicker steel box (B3) tend to present lower lateral-bearing capacity than the welded specimen R4W. Specimens R2W and R4W have similar skeleton curves, but for clarity only the curve for R4W is shown. Skeleton curves of the specimen tested with a coupler (B1PT80C) and without the coupler (B1PT80) are similar showing that the coupler did not affect the lateral capacity of the connection. Only the curve for B1PT80 is shown.

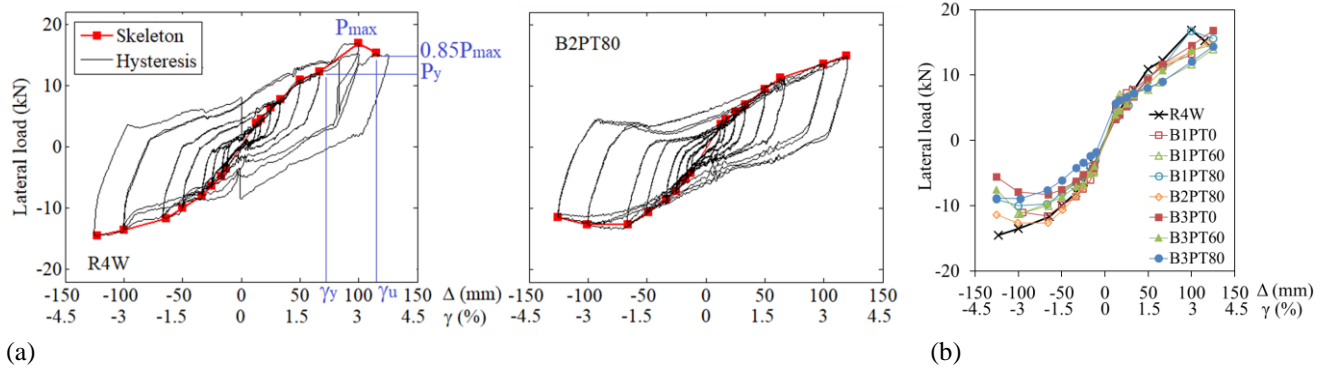


Figure 5. Hysteretic curve for R4W and B2PT80, (b) Skeleton curves.

Ductility ( $\beta$ ) is defined as the ratio of the failure drift ( $\gamma_u$ ) to the yield drift ( $\gamma_y$ ), as indicated in Eq. (1). As shown in Fig.5a, the failure drift is obtained when the lateral load drops to  $0.85P_{max}$ , where  $P_{max}$  is the maximum lateral load applied by the actuator. Except for specimens B3PT0 and B3PT60, none of the specimens experienced a reduction in the lateral load greater than or equal to 85% of the ultimate strength. Therefore, the failure drift was taken as the maximum drift ( $\gamma_{max}$ ). The yield drift corresponds to the drift at the yield load ( $P_y$ ), which is considered as two third of  $P_{max}$  [17,22]. Table 3 indicates the maximum lateral load ( $P_{max}$ ), yield load ( $P_y$ ), failure drift ( $\gamma_u$ ), yield drift ( $\gamma_y$ ), and ductility ( $\beta$ ) for all specimens in both positive and negative directions, except specimen R2W that was tested up to  $\pm 2\%$  drift only. The results show that ductility factor of the proposed connection varies between 1.70-3.93. The majority of the specimens presented ductility larger than 2.0, and in average the ductility obtained for the proposed PT connection is 2.58. It is worth to mention that because most of the specimens did not fail, the values of ductility presented in the table are conservative. Table 3 also includes the average energy dissipation ratio ( $E_{d,av}$ ) and average damping ratio ( $\xi_{av}$ ), both will be further discussed in this paper.

$$\beta = \gamma_u / \gamma_y \quad (1)$$

Table 3. Mechanical parameters, energy dissipation ratio and damping ratio.

Specimen	Loading direction	$P_{max}$ (kN)	$P_y$ (kN)	$\gamma_u$ (%)	$\gamma_y$ (%)	$\beta$	$E_{d,av}$	$\xi_{av}$
R4W	(+)	16.9	11.3	3.40	1.63	2.09	0.95	0.15
	(-)	14.5	9.6	3.70	1.42	2.60		
B1PT0	(+)	13.2	8.8	3.00	1.27	2.37	1.00	0.16
	(-)	11.6	7.7	2.80	0.81	3.45		
B1PT60	(+)	14.0	9.3	3.70	2.06	1.79	1.44	0.23
	(-)	11.3	7.5	3.00	1.40	2.14		
B1PT80	(+)	16.8	11.2	3.70	1.94	1.91	1.36	0.22
	(-)	10.0	6.7	3.70	1.05	3.52		
B1PT80C	(+)	14.8	9.8	3.70	1.51	2.46	1.33	0.21
	(-)	11.5	7.7	3.70	1.32	2.79		
B2PT80	(+)	14.9	9.9	3.70	1.59	2.32	1.12	0.18
	(-)	12.6	8.4	3.70	0.99	3.74		
B3PT0	(+)	16.9	11.2	3.70	1.90	1.95	1.41	0.22
	(-)	8.3	5.5	3.25	0.83	3.93		
B3PT60	(+)	14.7	9.8	3.70	1.76	2.10	1.29	0.21
	(-)	11.2	7.5	3.31	1.12	2.95		
B3PT80	(+)	14.4	9.6	3.70	2.18	1.70	1.40	0.22
	(-)	8.9	5.9	3.70	1.44	2.57		

### Stiffness degradation

Stiffness degradation is referred to the gradually loss of stiffness when a structural element is subjected to cyclic loading. Secant stiffness, as indicated in Fig. 6a, is defined in this paper as the ratio of the lateral load to the peak displacement applied at each set of cycles. As the displacement increases the secant stiffness tends to decrease, indicating stiffness degradation. Fig. 6b shows the secant stiffness ( $K$ ) obtained for each specimen at each set of cycles. It is observed that PT specimens with steel box B1 and B2 tend to develop higher initial stiffness than the welded one. To evaluate the stiffness degradation, Fig. 6c shows the normalized stiffness ( $K_{norm}$ ) defined as the ratio of the secant stiffness at each set of cycles to the secant stiffness of the first cycle. It is seen that specimens with PT connection present more pronounced stiffness degradation in comparison to the welded specimen. However, this is due to higher initial stiffness. The use of coupler did not affect the stiffness degradation rate of the specimen B1PT80C. For clarity, curves for specimens R2W and B1PT80C were not included.

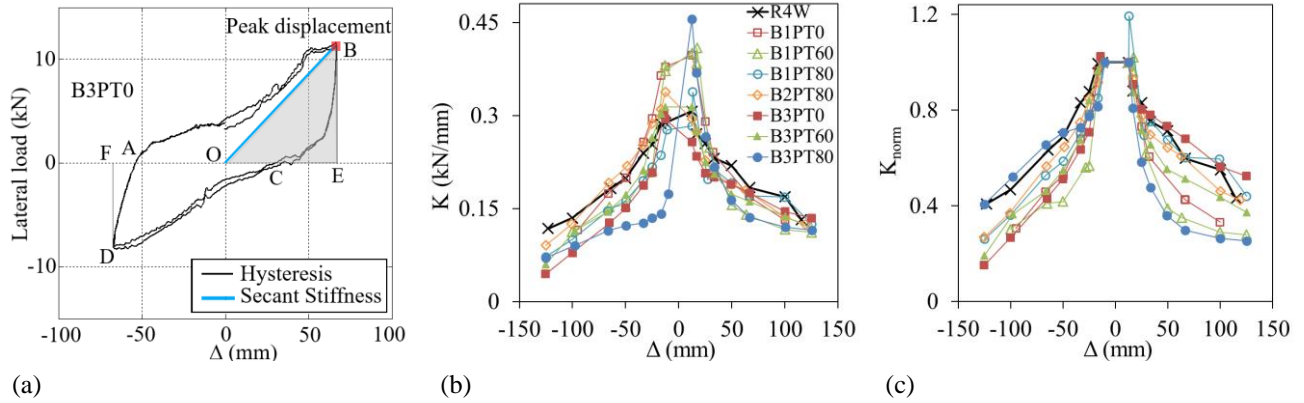


Figure 6. (a) Secant stiffness and hysteresis, (b) Secant stiffness, (c) Normalized stiffness.

### Energy dissipation and damping ratio

An important parameter for seismic performance assessment is the energy dissipated during cyclic loading. The energy dissipation ratio ( $E_d$ ) and damping ratio ( $\xi$ ) are normally used to evaluate the energy dissipation capacity of the structural components and are computed according to Eq. (2) and Eq. (3), respectively.  $A_{ABCD}$  is the area within the hysteretic loop (i.e., the energy dissipated in one cycle) and  $A_{OBE+ODF}$  is the summation of the areas OBE and ODF, as indicated in Fig.6a. Energy dissipation factor is defined as the ratio of the dissipated energy to the potential energy at peak load, and greater values of  $E_d$  and  $\xi$  indicate a good seismic performance [15,17].

$$E_d = A_{ABCD}/A_{OBE+ODF} \quad (2)$$

$$\xi = E_d/2\pi \quad (3)$$

Fig. 7a and Fig.7b provides  $E_d$  and  $\xi$ , respectively, per set of cycle for PT specimens and the welded specimen R4W. Both energy dissipation ratio and damping ratio tend to increase with increasing displacement amplitudes. The average damping ratio ( $\xi_{av}$ ) and average energy dissipation ratio ( $E_{d,av}$ ) are indicated in Table 3. The damping ratio for the PT specimens is 0.21 in average, while for the welded specimen is 0.15. The results show that the PT connection has better energy dissipation capability than typical welded connection.

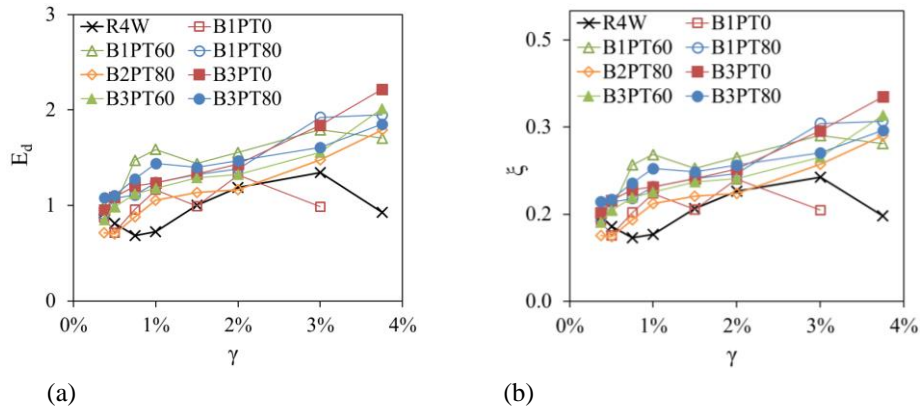


Figure 7. (a) Energy dissipation ratio, (b) Damping ratio.

## Eurocode classification

In this paper, the proposed connection is classified by stiffness and strength according to Eurocode 3 [23]. The classification boundaries suggested in Eurocode 3 is shown in Fig.8a. A steel connection is classified as rigid, nominally pinned, or semi-rigid by comparing its initial rotational stiffness with the beam stiffness. By strength, connections are categorized as nominally pinned if they have moment resistance smaller than  $0.25M_{p,beam}$ , or as full-strength connection if the moment resistance is greater than  $M_{p,beam}$ , where  $M_{p,beam}$  is the plastic moment of the beam. Finally, connections that are neither nominally pinned nor full-strength are categorized as partial-strength connections. Fig.8b shows the moment-rotation curves for the PT specimens and the welded specimen R4W; and the Eurocode boundaries. It can be seen that the proposed PT connection is categorized as partial strength semi-rigid connection. For clarity, the curve for specimen R2W was omitted. The moment was computed by multiplying the lateral force imposed by the actuator by the distance between the actuator and the floor beam (1763mm) and  $M_{p,beam}$  was taken as the plastic moment of the floor beam.

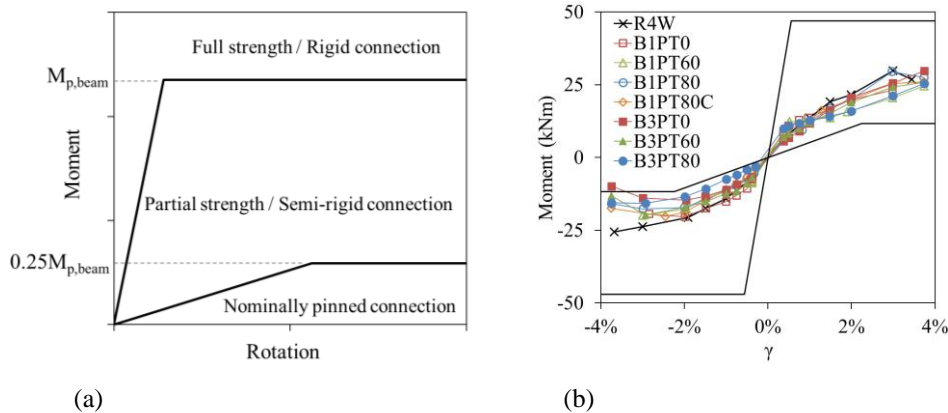


Figure 8. (a) Eurocode 3 classification, (b) Moment vs. drift curves.

## CONCLUSIONS

The present paper investigates the performance of a vertical post-tensioned (PT) connection for modular steel buildings. The connection is composed of a post-tensioned threaded rod installed inside the hollow steel columns, and a steel box inserted between two columns to transfer shear load between vertically consecutive modules. Eight full-scale subassemblies with the proposed PT connection were tested. In addition, two specimens were tested with typical welded connection. The results were compared, and the main conclusions are as follows:

- (1) All specimens were able to withstand up to 3% drift without weld fracture or buckling. Specimen tested with partial weld presented similar behavior to the fully welded specimen. The use of coupler did not affect the PT connection behavior.
- (2) Skeleton curves showed that specimens with steel box B1 and B2 tend to present similar lateral load-bearing capacity in comparison to connections with thicker steel box (B3). It is suggested that the thickness of the steel box should be limited to 1.5 times the thickness of the column. Additionally, specimens with PT connection presented greater ductility than the welded one.
- (3) In general, specimens with PT connection presented higher stiffness degradation rates than the welded specimen. However, most of the PT specimens presented higher initial secant stiffness, especially specimens with thinner steel box (B1).
- (4) Energy dissipation ratio and damping ratio obtained from hysteresis curves show that the proposed PT connection has greater energy dissipation capability than typical welded connection.
- (5) Moment-rotation curves were used to classify the connections by stiffness and strength. According to Eurocode 3 provisions, the proposed PT connection and the welded connection are classified as partial strength semi-rigid connections.

## ACKNOWLEDGMENTS

This paper is based upon work funded by the Natural Sciences and Engineering Research Council of Canada (NSERC) Discovery (2016-06290) and Engage (EGP 506929) Programs. The first author acknowledges the scholarship provided by National Council for Scientific and Technological Development (CNPq, 234888/2014-8). The authors would like to express their appreciation to NRB Inc. and Jerol Inc. Technologies who were collaborators in this project. Any opinions, findings,

conclusions and recommendations expressed here are those of the authors and do not necessarily reflect the views of the sponsors.

## REFERENCES

- [1] Lawson R.M., Ogden R.G., Bergin R. (2012). “Application of modular construction in high-rise buildings”. *J Archit Eng*, 18, 148–54.
- [2] Jellen A.C., Memari A.M. (2013). “The state-of-the-art application of modular construction to multi-story residential buildings”. In: *1st residential building design & construction conference*, Bethlehem, PA.
- [3] Ramaji I.J., Memari A.M. (2016). “Product architecture model for multistory modular buildings”. *J Constr Eng Manage*, 142(10), 1-14.
- [4] Gunawardena T. (2016). *Behavior of prefabricated modular buildings subjected to lateral loads*. Ph.D. thesis. Department of Infrastructure Engineering. University of Melbourne.
- [5] Lacey A.W., Chen W., Hao H., Bi K. (2018). “Structural response of modular buildings – an overview”. *J Build Eng*, 16,45–56.
- [6] Annan C.D., Youssef M.A., El Naggar M.H. (2009). “Seismic overstrength in braced frames of modular steel buildings”. *J Earthquake Eng*, 13,1–21.
- [7] Annan C.D., Youssef M.A., El Naggar M.H. (2009). “Experimental evaluation of the seismic performance of modular steel-braced frames”. *Eng Struct*,31,1435–46.
- [8] Fathieh A., Mercan O. (2016). “Seismic evaluation of modular steel buildings”. *Eng Struct*,122,83–92.
- [9] Ricles J.M., Sause R., Garlock M., Zhao C. (2001). “Posttensioned seismic-resistant connections for steel frames”. *J Struct Eng*,127(2),113–21.
- [10] Ricles J.M., Sause R., Peng S.W., Lu L.W. (2002). “Experimental evaluation of earthquake resistant posttensioned steel connections”. *J Struct Eng*,128(7),850–9.
- [11] Garlock M.M., Ricles J.M., Sause R. (2005). “Experimental studies of full-scale posttensioned steel connections”. *J Struct Eng*,131(3),438–48.
- [12] Garlock M.M., Sause R., Ricles J.M. (2007). “Behavior and design of posttensioned steel frame systems”. *J Struct Eng*,133(3),389–99.
- [13] Chi H., Liu J. (2012). “Seismic behavior of post-tensioned column base for steel self-centering moment resisting frame”. *J Constr Steel Res*,78,117–30.
- [14] Chen Z., Li H., Chen A., Yu Y., Wang H. (2017). “Research on pretensioned modular frame test and simulations”. *Eng Struct*,151,774–87.
- [15] Chen Z., Liu J., Yu Y., Zhou C., Yan R. (2017). “Experimental study of an innovative modular steel building connection”. *J Constr Steel Res*,139,69–82.
- [16] Chen Z., Liu J., Yu Y. (2017). “Experimental study on interior connections in modular steel buildings”. *Eng Struct*, 147,625–38.
- [17] Deng E.F., Zong L., Ding Y., Dai X.M., Lou N., Chen Y. (2018). “Monotonic and cyclic response of bolted connections with welded cover plate for modular steel construction”. *Engineering Structures*,167,407–419.
- [18] Sanches, R., Mercan, O., Roberts, B. (2018). “Experimental investigations of vertical post-tensioned connection for modular steel structures”. *Engineering Structures*, 175, 776-789.
- [19] American Institute of Steel Construction – AISC (2005). *Seismic provisions for structural steel buildings: ANSI/AISC 341-05*, Chicago, Illinois.
- [20] American Society for Testing Material – ASTM-A370 (2015). *Standard test methods and definitions for mechanical testing of steel products: ASTM-A370-15*, USA.
- [21] McMaster-Carr.<<https://www.mcmaster.com>>[accessed on June 23, 2018].
- [22] Faella C., Piluso G., Rizzano G (2000). *Structural steel semirigid connections: theory, design and software*. Boca Raton, Fla: CRC Press.
- [23] Eurocode 3 (2005). *Design of steel structures-Part 1–8: Design of joints. EN 1993-1-8:2005*. European Committee for Standardization, Brussels.